Manila Journal of Science ***14*** *(2021), pp. 86–103*

Evaluation of Land Use Land Cover Change due to Urbanization in Mactan Island, Cebu, Using Landsat Data

Dionde C. Clarin* Danilo T. Dy, and Annie G. Diola
Department of Biology, University of San Carlos, Cebu City, Philippines

*Corresponding Author: android00dionde@gmail.com

ABSTRACT

Rapid urbanization is occurring at an unprecedented rate in recent human history and is having a marked effect on the natural functioning of ecosystems. Changes in land use/land cover (LULC) due to urbanization is proceeding more quickly in ASEAN (Association of Southeast Asian Nations). This study aims to quantify LULC changes in Mactan Island (Central Philippines) using remote sense data from Landsat 7 ETM+ for the year 2000 and Landsat 8 OLI for the year 2018. The Semi-Automatic Classification Plugin in QGIS was used in analyzing and processing of Landsat data. Fragmentation patterns were identified, and the effect of LULC change on land surface temperature was evaluated. Overall accuracies of Landsat-derived land use data were 86.2% and 86.4% for the years 2000 and 2018, respectively. Results showed that the built-up class had increased to about 31.3% while other classes such as vegetation (25.8%), bare soil (7.3%), and water bodies (74.4%) had decreased. The mean land surface temperature increased by about 2.9 °C from 2000 to 2018. Vegetation patches increased from 515 in 2000 to 862 patches in 2018, suggesting the degree of fragmentation and the extent of subdivision of the landscape. LULC has significantly changed from the year 2000 to 2018. Fast urbanization in the island had led to fragmentation of vegetation and an increase to land surface temperature. The results of this study provide additional information that is important to the urbanization process in Mactan Island and can be used further to investigate the effect of LULC on local climate change in the future.

Keywords: urbanization, land cover change, Landsat, GIS

INTRODUCTION

Urbanization is one of the biggest anthropogenic activities that have caused the loss of arable land, habitat destruction, and the decline of natural vegetation (Alphan, 2003; Dewan & Yamaguchi, 2009; Lopez et al., 2001). It is occurring at an unprecedented rate in recent human history and having a marked effect on the natural functioning of ecosystems (Turner, 1994). It is projected that land use/land cover (LULC) changes due to human activities and the development of megacities by the year 2020 will be located in developing countries (World Bank, 2007). To mitigate haphazard development of urban space, it is important to assist government officials of affected cities with regards to their planning strategies in tackling potential risks and adverse effects of urbanization (Son & Thanh, 2017). Maps of vegetation, land surface temperature (or LST), and LULC can provide a "bird's-eye view" and concrete evidence of urbanization. The practical application of remote sensing (RS) and a geographic information system (GIS) comes in handy in assessing LULC change and LST. The interpretation and classification of RS data are very useful for estimating the spatial pattern and rate of urban growth with time. The physical pattern of urban growth can be identified, and the characteristics of these patterns such as infill, expansion, and outlying (Wilson et al., 2003) can provide an overview on the spatial distribution and arrangement of built environments and identify "pockets of urbanization." Estoque et al. (2017) conducted a study on the relationship between LST and the abundance and spatial pattern of impervious surface and green space in the megacities of Southeast Asia, including Manila. The methods of processing Landsat data for LULC assessment were standard. However, using an open-source software like the Semi-Automatic Classification Plugin (SCP) in QGIS in this study is new and currently limited in growing urban centers in the Philippines. Recent studies about RS were using commercial software such as ENVI, ERDAS Imagine, ArcGIS, etc., which is very expensive. Open-source and new technologies had paved way to researchers in quantifying and assessing anthropogenic impacts on the environment. Mactan Island (Lapu-Lapu City mainland and Cordova) is a highly urbanized area in Central Visayas, Philippines. In recent years, the island has experienced rapid expansion of urban built-up and tourism-related developments. The effects of traffic congestions, flooding, dense population, and housing development in Mactan Island are unique (i.e., limited space and fast industrialization) compared to other cities in the province of Cebu and Central Visayas. In this study, we quantified the LULC changes in Mactan Island between 2000 and 2018 using Landsat data. Fragmentation patterns were also assessed for the green spaces/urban vegetation. Lastly, the effects of LULC change on LST were evaluated.

MATERIALS AND METHODS

The Study Area

Mactan Island (Fig. 1) is a densely populated island located about few kilometers from Cebu Island (Central Philippines). The island is located between 123°54'4.49"E longitude, 10°20'2.57"N latitude and 124°2'45.00"E longitude, 10°14'43.66"N latitude. It consists of the mainland Lapu-Lapu City and the municipality of Cordova with a land area of approximately 6,244.5 ha. The island is dominated mostly by industrial and residential areas. Economic zones such as the Mactan Export Processing Zone (MEPZ) I and II and Cebu Light Industrial Park (CLIP) serve as the base operations of various multinational companies. The Mactan-Cebu International Airport is located in the island and serves as the gateway for domestic and international air travel. It has two bridges that link to Cebu Island, and a third bridge (from Cordova to Cebu) is undergoing construction. The island topography is generally flat, and some areas are slightly elevated.

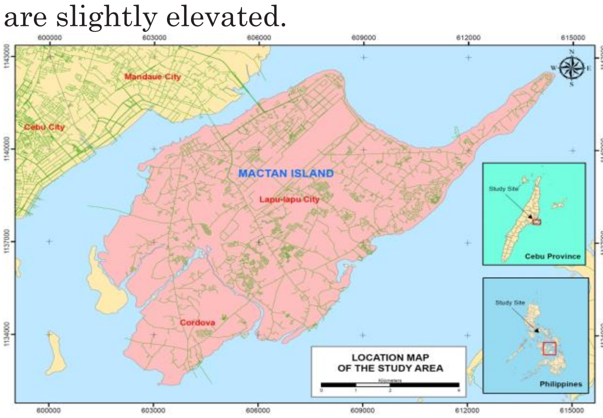

Figure 1. Location map of study area. Map showing its road networks and proximity to Cebu City and Mandaue City (data source: GADM, 2012). The map projection is in UTM Zone 51N.

GADM Collection

The methods used in this study generally involved the following steps: data collection, preparation, processing, analysis, and assessment of the data collected (see Figure 2). Landsat time series data were collected for the years 2000 and 2018 from https://glovis.usgs.gov with Worldwide Reference System (WRS) path 113 and row 053 (Global Visualization [GloVis] Viewer, 2005). For 2000 data, Landsat 7 images were used since Landsat 8 has only images from 2013 onwards. Scenes with minimum or without cloud cover were considered in choosing the appropriate satellite images in this study. We used Landsat Level-2 or Surface Reflectance data products except for scene 2018 of Landsat 8, where we used the Level-1 data since no Level-2 data were available. The availability of Landsat Surface Reflectance High Level Data Products was prioritized since it can provide better and more accurate land cover classifications. However, if these data are not available, the conversion to surface reflectance using the Dark Object Subtraction 1 method was done to provide significant enhancement to the original Landsat image, particularly for the supervised classification of old images (Congedo, 2016). This study uses Landsat data with 30-m-per-pixel resolution and applies it in the scale ranges between 1:50,000 and 1:100,000 (Bhatta, 2010; Sabins, 1996).

Data Analysis and Processing

We used QGIS 3.0 (QGIS Development Team, 2015) and the SCP in QGIS to analyze and process the Landsat data. Landsat images were projected using UTM Zone 51N projection with WGS84 datum and clipped within the desired study area. Dark Object Subtraction was used for atmospheric corrections. It is worth pointing out that the accuracy of image-based techniques is generally lower than physically based corrections, but they are very useful when no atmospheric measurements are available as they can improve the estimation of land surface reflectance (Chavez, 1996).

LULC classification went through unsupervised and supervised classification procedures. Identified spectral signatures of land covers were defined through a Macroclass ID, a group of regions of interest (ROIs) having different Class IDs, which is useful when one needs to classify materials that have different spectral signatures in the same land cover class. For instance, one can identify a grass or trees Class as a vegetation Macroclass (i.e., Class = grass or trees, Macroclass = vegetation). Multiple Class IDs can be assigned to the same Macroclass ID, but the same Class ID cannot be assigned to multiple Macroclass IDs. Table 1 shows the different Classes assigned to a Macroclass.

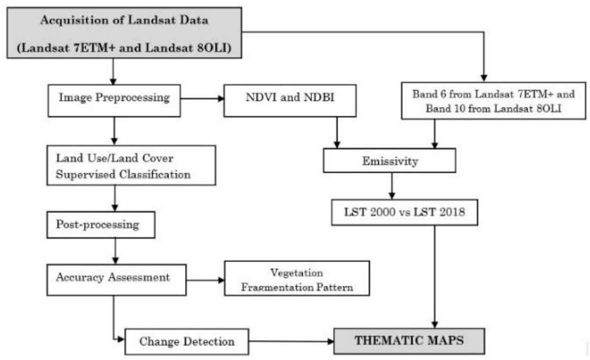

Figure 2. Data processing flow diagram showing the summary of procedures in generating LULC maps and evaluation of LST from Landsat data.

The Maximum Likelihood classification algorithm in SCP was used. The classification of land cover in urban areas was more challenging because of landscape heterogeneity and the amount of threshold in the environment that creates confusion in identifying the accurate cover of an area. In order to increase classification accuracy and reduce classification error caused by confusion in spectral response of specific classes, the generalized images were spatially reclassified and refined for classification validation (Congedo, 2016).

Table 1. Different Class Names Assigned to a Macroclass

Macroclass Name	Class Name
Vegetation	Trees, grass, shrubs
Built-up	Buildings, roads
Bare soils	Barren land, excavation sites
Water bodies	Rivers, seas

Data reclassification was applied to properly consolidate the different LULC types. Reclassification was carried out using reference data (e.g., roads, boundaries) and Google Earth, which provided clear present image-based information and some historical imageries that were very useful in reclassification.

Change Detection

Classification results were compared to quantify the changes that occurred in different years (2000 and 2018) using change detection analysis in SCP. Two change detection statistics were obtained from independent classified images. "From-to" change information matrices and maps were presented to show the main gains and losses in each category.

Fragmentation Pattern

In identifying fragmentation patterns of vegetation, landscape metrics were calculated using LecoS (Landscape Ecology Statistics), a plugin for QGIS (Jung, 2016). A landscape is represented as a collection of discrete patches (Leitão et al., 2006). The LecoS plugin identifies patches by class to calculate metrics (i.e., Land Cover, Landscape Proportion [LP], Number of Patches, Greatest Patch Area, Mean Patch Area). Fragmentation pattern analysis using LecoS was performed to identify patches of class vegetation and calculate several landscape metrics. The proportional abundance of vegetation class obtained through LP indicates changes in area.

Vegetation and Built-Up Areas

The normalized difference vegetation index (or NDVI) provided information about the density of vegetation, crop production, and measurement of surface radiant temperature (Aboelnour & Engel, 2018) while the normalized difference built-up index (or NDBI) was used to investigate the extent of imperviousness and built-up areas and can highlight the urban distribution with a typically higher reflectance in the short-wave infrared region band than in the near-infrared one (Aboelnour & Engel, 2018; Alwahiti & Mitsova, 2016). NDVI and NDBI were calculated using the following formulas:

$$NDVI = (Band\ 5 - Band\ 4)/(Band\ 5 + Band\ 4) \quad (1)$$

$$NDBI = (SWIR - NIR)/(SWIR + NIR) \quad (2)$$

where

NIR = Near Infrared (Band 4 for Landsat 7 and Band 5 for Landsat 8); and

SWIR = Short Wavelength Infrared (Bands 5 and 7 are the SWIR for Landsat 7, while Bands 6 and 7 are the SWIR for Landsat 8).

LST

Before at-sensor reflectance can be determined for Landsat 7 ETM+ images, the radiance was first calculated using digital number (DN) values. The following equation was used to convert DN to radiance units:

$$L(\lambda) = GainxDN + Offset \quad (3)$$

where

L(λ) is at sensor;
Gain is the slope of the radiance/DN conversion function;
DN is the digital number of a given pixel; and
Offset (or bias) is the intercept of the radiance/DN conversion function.

For this study, we used a land cover classification for the definition of the land surface emissivity of each class (Weng et al., 2004):

$$e = a + b \times ln(landcover) \quad (4)$$

where a and b were obtained by regression analysis based on the largest data set (Aboelnour & Engel, 2018; Faridatul, 2017).

It should be noted that the correct evaluation of LST was constrained to an accurate estimation of surface emissivity (Aboelnour & Engel, 2018). The estimation of LST (denoted as T in the equation) was calculated as

$$T = T\,B/[1 + (\lambda * T\,B/c\,2) * ln(e)] \quad (5)$$

where

λ = wavelength of emitted radiance;
$c_2 = h*c/s = 1.4388*10^{-2}$ m K;
h = Planck's constant = $6.626*10^{-34}$ J s;
s = Boltzmann constant = $1.38*10^{-23}$ J/K;
c = velocity of light = $2.998*10^{8}$ m/s; and
e = emissivity.

The calculation of LST for Landsat 7 ETM+ images was processed in units of absolute radiance using 32-bit floating-point calculations or DNs. These values were converted to spectral radiance scaling factors provided in the metadata file (USGS, 2016):

$$L_\lambda = M_L * Q_{cal} + AL \quad (6)$$

where

L_λ = Spectral radiance ($W/(m_2*sr*\mu m)$);
M_L = Radiance multiplicative scaling factor for the band (RADIANCE_MULT_BAND_n from the metadata);
AL = Radiance additive scaling factor for the band (RADIANCE_ADD_BAND_n from the metadata); and
Q_{cal} = L1 pixel value in DN.

The estimation of LST for Landsat 8 OLI images was calculated the same as with the Landsat 7 formula. The emissivity (e) was estimated using land cover classification with the same formula used in Landsat 7 ETM+ since it is also preferably used in some other studies (Aboelnour & Engel, 2018; Sobrino et al., 2004). Kelvin values were converted to Celsius using the following equation:

$$°C = T - 273.15 \quad (7)$$

Accuracy Assessment

Sampling points were generated randomly and validated using Google Earth Imageries and actual field surveys. We used a stratified sampling design to increase the sample sizes for small areal proportions to reduce standard errors of the class-specific accuracy estimate for other classes. The number of samples (N) for each class was calculated using the following formula (Olofsson et al., 2014):

$$N = (\sum i = 1\ (W_i - S_i)/S_o)2 \quad (8)$$

where

N = total number of classes;
W_i = mapped area proportion of class i;
S_i = standard deviation of stratum i; and
S_o = expected standard deviation of overall accuracy.

The procedure requires some conjectures about overall accuracy and user's accuracy of each class (Congedo, 2016). To stratify samples, we conjectured the user's accuracy and standard deviations of strata (Olofsson et al., 2014). A rough approximation is to consider the mean value between equal distribution ($N_i = N/c$) and weighted distribution ($N_i = N*W_i$), which is $N_i = (N/c + N*W_i)/2$. Once the sampling data were stratified, single pixel training areas (ROIs) were created, and the attribution of a land cover class based on photo-interpretation of each ROI (Congedo, 2016) was made. Standard accuracy assessment metrics were performed using SCP to calculate overall accuracy, producer's accuracy, and user's accuracy using the following formula:

$$Overall\ accuracy\ (\%) = Total\ correct\ class\ ID / Total\ samples \times 100$$
$$Producer's\ accuracy\ (\%) = 100\% - error\ of omission\ (\%)$$
$$User's\ accuracy\ (\%) = 100 - error\ of\ commission\ (\%)$$

These processes were calculated statistically according to the area-based error matrix (Olofsson et al., 2014) where each element represents the estimated area proportion of each class.

RESULTS

Accuracy Assessment

Tables 2 and 3 contain the percentage of each class that was divided by 100 to get the required W_i. The expected standard deviation is S_o = 0.01 and conjectures the S_i values.

The allocated samples for the year 2000 were 151 and for the year 2018 were 150. Tables 4 and 5 show the estimated allocation of samples in every class. Tables 6 and 7 contain the area-based error matrix for the years 2000 and 2018.

Table 8 contains the percent producer, user, and overall accuracies including 95% confidence interval (CI) area per class after data processing. The percent overall accuracy of 86.2 for year 2000 and 86.4 for year 2018 are acceptable if compared to other studies (e.g., Rahman & Saha, 2007; Tao & Xin, 2004).

LULC Classification and Change Detection

The general direction of urbanization as shown in the built-up class (Fig. 3) can be seen emanating from the city/municipal centers where malls, public markets, schools, churches, and public amenities are located. For Lapu-Lapu City, the direction of built-up sprawl was moving southeast starting from the barangays of Poblacion, Pajo, Pusok, Ibo, Gun-ob, and Basak. Built-up areas in the southeastern part of the city recently sprung due to limited spaces near the city proper. The direction of built-up sprawl in the municipality of Cordova, however, is observed as spiraling or circulating outward from the municipal proper

Table 2. Conjectured Standard Deviations on Year 2000

	Land Cover Class	Class Number	Area (m²)	%	W_i	S_i	$W_i{*}S_i$
2000	Built-up	1	20,450,700	32.45	0.324508	0.20	0.06
	Vegetation	2	30,085,200	47.74	0.477386	0.10	0.05
	Bare soil	3	6,269,400	9.95	0.099482	0.06	0.01
	Water	4	6,215,400	9.86	0.098625	0.04	0.00
	Total						**0.123**

Mactan Island shows a "strip" or "ribbon" development, in which residences or commercial properties line roads extending outward from urban centers (Tsai, 2005). Homes arranged along rural highways present hazards related to traffic safety; commercial strips composed of fast-food chains and large retail stores cater to automobile access and are often fronted by expansive parking lots.

The increasing areas of built-up cover have a significant effect on the magnitude of LST, and while these areas increased, vegetation in the urban surroundings decreased over the years. This was observed during the field validation as impervious pavements, concrete structures, and asphalt roads. A matrix showing land cover conversion from 2000 to 2018 of Mactan Island (Central Philippines) showed the greatest change was the built-up class (Table 9).

Table 3. Conjectured Standard Deviations on Year 2018

	Land Cover Class	Class Number	Area (m²)	%	W_i	S_i	$W_i{*}S_i$
2018	Built-up	1	29,778,300	47.27	0.472739	0.13	0.06
	Vegetation	2	23,976,900	38.06	0.38064	0.10	0.04
	Bare soil	3	5,636,700	8.95	0.089484	0.22	0.02
	Water	4	3,599,100	5.71	0.057137	0.06	0.003
	Total						**0.123**

For 2018, $N = (0.12267/0.01)^2 = 150$.

Table 4. Year 2000 Allocated Samples for Each Class

Land Cover Class	Weighted	Equal	Mean
Built-up	49	38	43.14
Vegetation	71	38	54.62
Bare soil	15	38	26.25
Water	15	38	26.18
Total			**151**

Table 5. Year 2018 Allocated Samples for Each Class

Land Cover Class	Weighted	Equal	Mean
Built-up	71	38	54.35
Vegetation	57	38	47.42
Bare soil	13	38	25.53
Water	9	38	23.10
Total			**150**

Table 6. Area-Based Error Matrix for Year 2000

	Built-Up		Vegetation		Bare Soil		Water Bodies	
	Sample Counts	Error	Sample Counts	Error	Sample Counts	Error	Sample Counts	Error
Built-up	41	0.1231	6	0.0180	2	0.0060	0	0.0000
Vegetation	2	0.0060	68	0.2044	2	0.0060	0	0.0000
Bare soil	3	0.0090	1	0.0030	11	0.0331	0	0.0000
Water bodies	0	0.0000	0	0.0000	1	0.0030	14	0.0417

Table 7. Area-Based Error Matrix for Year 2018

	Built-Up		Vegetation		Bare Soil		Water Bodies	
	Sample Counts	Error	Sample Counts	Error	Sample Counts	Error	Sample Counts	Error
Built-up	60	0.1810	4	0.0121	7	0.0211	0	0.0000
Vegetation	8	0.0242	48	0.1452	1	0.0030	0	0.0000
Bare soil	3	0.0094	0	0.0000	10	0.0312	0	0.0000
Water bodies	0	0.0000	0	0.0000	0	0.0000	9	0.0259

Table 8. Producer, User, and Overall Accuracies Including 95% CI Area per Class (m^2) for Years 2000 and 2018

	Built-Up	Vegetation	Bare Soil	Water Bodies
Year 2000				
Producer accuracy	89.1176	90.6748	68.8016	100.0000
User accuracy	83.6735	94.4444	73.3333	93.3333
95% CI	85.62	91.65	65.21	86.00
Overall accuracy	**86.20**			
Year 2018				
Producer accuracy	84.5070	84.2105	76.9231	100.0000
User accuracy	84.3586	92.3285	56.3659	100.0000
95% CI	87.94	87.20	66.07	100
Overall accuracy	**86.41**			
95% CI area per class (m^2)				
Year 2000	2,760,599	2,614,855	2,324,170	812,146
Year 2018	3,596,569	2,798,390	2,609,639	0

Table 9. A Matrix Showing Land Cover Conversion From 2000 to 2018 of Mactan Island (Central Philippines)

			2018				
	Class Area (ha)	**Built-Up**	**Vegetation**	**Bare Soil**	**Water Bodies**	**NO CHANGE**	**Difference**
2000	Built-up	1,461.69	425.61	152.64	5.22	1,461.69	932.58
	Vegetation	1,191.51	1,617.75	185.31	12.51	1,617.75	−616.23
	Bare soil	222.93	216.90	154.62	10.44	154.62	−41.31
	Water bodies	101.61	130.59	71.01	341.73	341.73	−275.04
						3,575.79	
	Total change 2008–2018	1,516.05	773.10	408.96	28.17	**2,726.28**	
	2018 LAND COVER	2,977.74	2,390.85	563.58	369.90		

Note. The results were extracted from Landsat data using the Semi-Automatic Classification Plugin algorithms of QGIS 3.0.

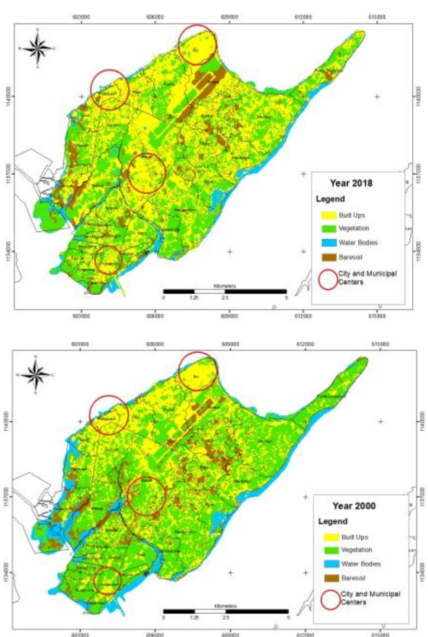

Figure 3. Spatial distribution of land cover classes in Mactan Island (Central Philippines) from 2000 to 2018. The results were extracted from Landsat data using SCP algorithm of QGIS 3.0.

The change rate of land cover classification (i.e., total of 12 classes) was calculated from year 2000 to 2018 (as shown in Table 10). The largest change rate increase was in vegetation to built-up class in the amount of about 143.82 ha (or 9.43%), as shown in Table 10. Vegetation cover had a decreasing rate of about −229.68 ha (−23.94%) followed by the bare soil class with a change rate of −165.15 ha (−66.55%).

Table 11 shows the different landscape metrics of fragmentation analysis. From 48% LP, class vegetation decreased to 38% LP suggesting some degree of urbanization. The proportional decrease of the vegetation class if analyzed together with the increase in the built-up class suggests urban expansion. Meanwhile, vegetation patches had increased from 515 to 862 patches in 2018 suggesting the degree of fragmentation and the extent of subdivision of the landscape. The area of the greatest patch area went down from 1,495.5 ha to 332.3 ha. The mean patch area and land cover area of vegetation had also decreased from

2000 to 2018 indicating some degree of environmental degradation.

LST, NDVI, and NDBI

The spatial distribution of LST in the year 2000 is shown in Figure 4. Bare soil had the highest mean LST (25.6 °C−28.54 °C) and high-density built-up areas (25.8 °C−28.17 °C) while water bodies had the lowest (20.91 °C−24.32 °C). There was a mean temperature difference of 2.9 °C from 2000 to 2018. We also presented NDVI and NDBI indices (Figures 5 and 6) derived from Landsat 7 and 8 bands. Higher NDVI values correspond to dense vegetation areas. In general, decreasing vegetation covers and increasing impervious surfaces modified thermal behavior. Thus, there is an inverse relationship between NDVI and NDBI indices. Table 12 shows the correlation values between LST, NDBI, and NDVI, and presented in Figures 7 and 8 is the regression analysis of the values derived from pixel values of LST and the two indices.

Table 10. Change Rate of Land Cover Conversion From 2000 to 2018 of Mactan Island (Central Philippines)

Transition	Area (ha)	%
Built-up to vegetation	−229.68	−23.94
Built-up to water bodies	7.47	27.13
Built-up to bare soil	50.22	18.34
Vegetation to built-up	143.82	9.43
Vegetation to water bodies	−0.63	−1.08
Vegetation to bare soil	26.01	5.87
Bare soil to built-up	−51.84	−15.73
Bare soil to vegetation	−94.32	−25.13
Bare soil to water bodies	15.57	20.15
Water bodies to built-up	−10.89	−6.59
Water bodies to vegetation	−73.08	−41.67
Water bodies to bare soil	−165.15	−66.55

Table 11. Landscape Metrics Computed for Vegetation Class (for Year 2000 and 2018) for Mactan Island, Central Philippines

Metrics	2000	2018
Landscape proportion	48%	38%
Number of patches	515.0	862.0
Greatest patch area (ha)	1,495.5	332.3
Mean patch area (ha)	5.84	2.77
Land cover area (ha)	3,007.1	2,390.9

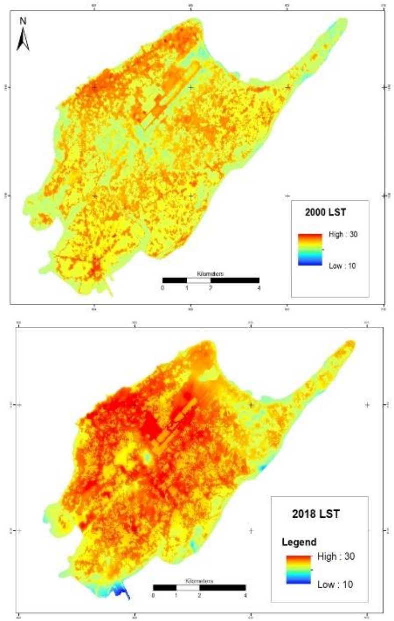

Figure 4. Spatial distribution of land surface temperature (LST) in Mactan Island (Central Philippines) for the years 2000 and 2018. The results were extracted from the SCP plugin of QGIS 3.0.

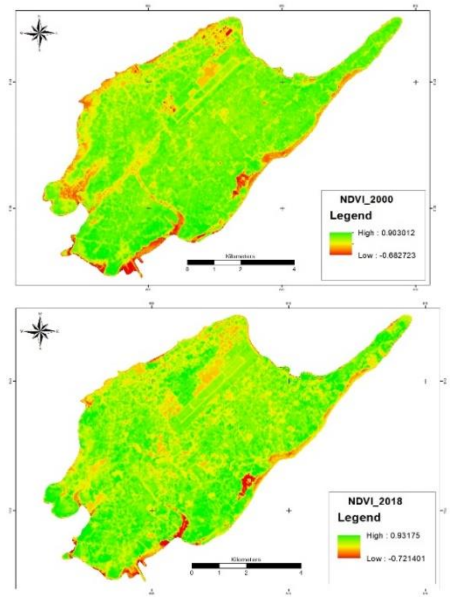

Figure 5. Normalized difference vegetation index (NDVI) maps of Mactan Island (Central Philippines) for the years 2000 and 2018.

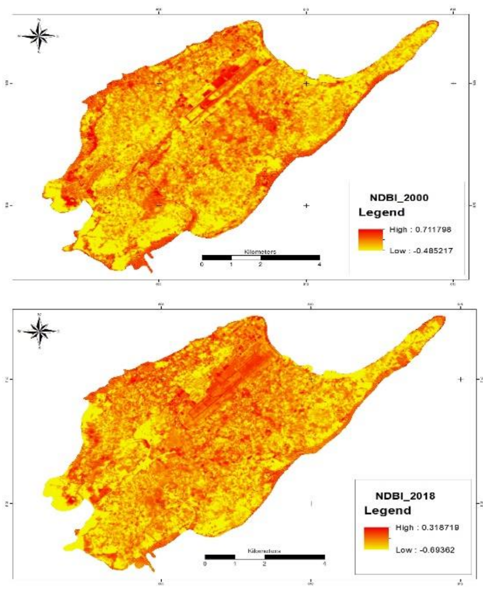

Figure 6. Normalized difference built-up index (NDBI) maps of Mactan Island (Central Philippines) for years 2000 and 2018.

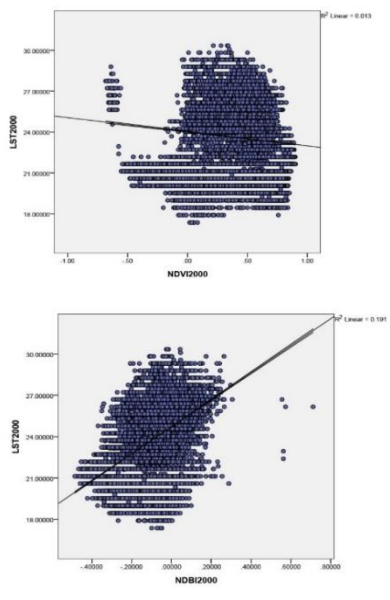

Figure 7. Correlation of land surface temperature (LST) versus normalized difference vegetation index (NDVI) and normalized difference built-up index (NDBI) for the year 2000 of Mactan Island (Central Philippines).

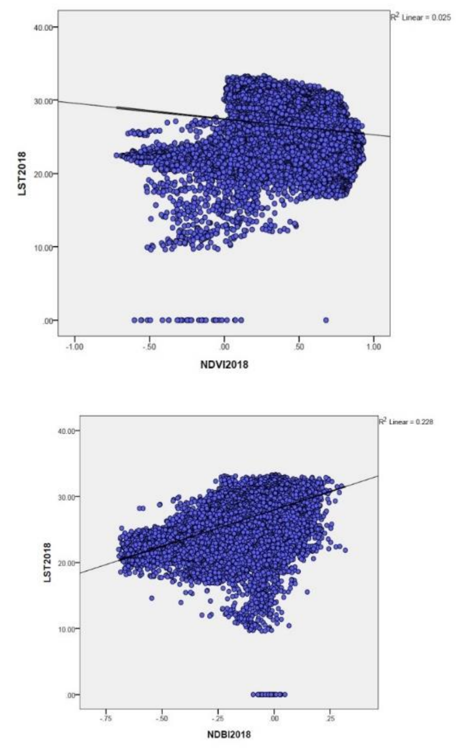

Figure 8. Correlation of land surface temperature (LST) versus normalized difference vegetation index (NDVI) and normalized difference built-up index (NDBI) for the year 2018 of Mactan Island (Central Philippines).

DISCUSSION

The application of multitemporal Landsat data provides a valuable tool in monitoring LULC change. Accuracy assessment results showed that the classification at the given scale is acceptable to provide accurate representation of the classified land cover when referenced to actual on-the-field data. The spectral confusion and mixed-pixel problems between built-up areas and other land-cover types such as bare soil and terrestrial vegetation in each studied year complicated the classification process, but with the help of historical images from Google Earth, the correct representation of each land cover was confirmed.

Mactan Island, being a fast-growing urban center in Central Philippines, exhibits both positive and negative impacts of urbanization. Urban growth in the island provides higher economic production and opportunities for the underemployed and unemployed and boosts tourism. However, its negative impacts necessitate regulations. There is already decreased vegetation cover due to increasing built-up development and increased urban heat island (UHI) effect. The accumulation of industrial and domestic wastes, water pollution, and other environmental impacts that can affect the sustainability of urban areas should not be overlooked (FAO & FAPDA, 2015).

The change in LST from 2000 to 2018 is a manifestation of the UHI effect (EPA, 2008) in Mactan Island. UHI has a significant and negative impact on the urban ecosystem and quality of life. Negative impacts include increased energy consumption, elevated emissions of air pollutants and greenhouse gasses, compromised human health and comfort, and degraded water quality (EPA, 2008).

In a growing urban system, vegetation cover undergoes alteration, replaced with built-up covers from simple houses to subdivisions, commercial buildings, and industrial zones. In the span of 18 years, the vegetated areas in Mactan Island decreased and became more fragmented. Based on the result, the LST had increased over time along with the decline in vegetation cover. The conversion of vegetation to urban built-up areas can be observed near the city/municipal center, high-density populated residential zones, the industrial zone, and the airport. This finding agreed with the results of Busato et al. (2014) and Wu et al. (2019).

Impervious pavements, concrete structures, and asphalt roads that efficiently absorb heat from sunlight and reradiate it as thermal infrared radiation could lead to modifications of the land surface characteristics such as albedo and evapotranspiration (EPA, 2008; Oke, 1982). Buildings block air that cools the surrounding and is associated with the production of heat from air conditioning and refrigeration systems. In effect, this causes discomfort for the people living in the urban area (Jacquin et al. 2008). If temperatures will continue to rise, it is possible that the feeling of discomfort due to heat will increase in barangays that are located very near urban centers of Lapu-Lapu City and Cordova.

NDBI, which represents the indices of impervious surface in built-up cover, positively correlates with LST. Hence, built-up areas with less vegetation should experience warmer temperature. Many studies (Abdollahi & Ning, 2000; Akbari et al., 1996, 2001; Miller & Small, 2003; Nowak et al., 2000; Wagrowski & Hites, 1997) have shown that abundance and distribution of vegetation play an important role in controlling temperature in an urban environment. Spatial variations in vegetation cover have a direct impact on solar energy flux, evapotranspiration, microclimate, and air circulation in the urban environment (Miller & Small, 2003).

The population grew because of the substantial influx of people to industrial centers. The population of Mactan Island increased by about 86% from 2000 (251,051) to 2015 (467,824; PSA, 2000, 2015). Mactan Island hosts three industrial economic zones, namely, Mactan Export Processing Zone 1 (MEPZ 1), Mactan Eco-zone 2 (MEZ 2), and CLIP. These transient workers came from different provinces not only in Cebu but also in other parts of the country. As more and more people settled for the convenience and access to their workplace, residential and subdivision developments also increased.

The island is also experiencing legal disputes causing people to leave vacant spaces within the inner city. This has led to the outward growth from the city centers. As a consequence, residential developments spread wider since transient workers preferred convenience in going to their job sites, which are mostly in the industrial economic zones. Though Mactan Island is relatively flat geologically, there is a high risk to high-rise buildings and condominiums due to the presence of sinkholes. Thus, horizontal development is preferred. It is expected that years from now, more vacant lots will be converted to built-up housing at the expense of vegetation cover. This development should be tempered by increasing available green areas to reduce local temperature (Takebayashi & Moriyama, 2007) and mitigate the effect of UHI (Susca et al., 2011). Surely, there are still small patches of lands along pavements, urban sprawls, and roundabouts that can be vegetated. Hence, policy makers should be aware and should provide green spaces (vegetated) as much as possible so as to make urban living livable. Allen et al. (2018) stressed the importance of understanding the role of public spaces and associated amenities of the neighborhood (i.e., parks, shops, schools, etc.) as population density increases in urban areas. According to the paper, local government units must acknowledge and incorporate into urban planning policy and strategy directives the community's sense of enhanced livability towards a successful path for urban sustainability.

Another consequence of urbanization that the island is experiencing is rapid flooding during heavy rains leading to overflowing of the water drainage systems. In November 2016, more than a thousand households in Basak, Lapu-Lapu City, were affected by the flood that has not subsided for more than one month. Tropical storm "Urduja" (international name "Kai-tak") in December 2017 also brought a 15-cm flood in some barangays of Lapu-Lapu City. An increase in impervious surfaces in the city induces more total runoff volume.

The growing development of subdivisions and industrial infrastructures at the edge of the island can hinder the proper flow of drainages from barangays located at the center of the island. Since the urban development on the island is widely dispersed, it can cause more urban runoff, which may eventually pollute waterways (Lassila, 1999; Wasserman, 2000). Reclamation in some coastal parts of the island and changes in LULC resulted in the decline of vegetated areas and could also threaten mangrove communities.

Following Wilson et al.'s (2003) category of urban growth patterns, the changes in built-up covers in Lapu-Lapu City can be described mostly as infill growth, especially in nearby city/municipal centers. Some areas in the southeastern part tended to exhibit an expansion type of growth. Patterns of built-up change in Cordova are mostly expansion and some infill growth. The vegetation class shows an outlying isolated and fragmented pattern of change both in Lapu-Lapu City and in Cordova. These patterns do not represent urban growth. Both the classes bare soil and water bodies showed mostly an infill pattern since they are surrounded by vegetation and built-up classes. It is the result mostly of excavation of land, dried ponds, reclamation, and construction. As cities develop, urban demand will increase with obvious impact on the sociospatial scale of its urban space (Twum & Ayer, 2019). Monitoring these complex change patterns demand critical attention from policy makers and academia towards the effective monitoring and modelling of complexities of urban settings (Ilieva, 2017; Tefft et al. 2017).

Degradation and fragmentation of vegetation in urban areas have negative impacts on human well-being including their quality of life and, to some extent, threaten urban sustainability. Ensuring adequate opportunities for people to be in contact with nature in their daily life could directly benefit health and happiness (Fuller et al., 2007; Mitchell & Popham, 2008; Pretty et al., 2007). Urban green spaces can be provided using existing LULC as has been done in Singapore. The presence of green parks, tree canopies along the roads, and plant boxes and gardens in subdivisions and condominiums suggests that vegetation can coexist with built-up development in urban cities. The amount of vegetation needed for an urban environment includes a mixture of quantitative and accessibility standards as well as qualitative standards taking into consideration some variations in its structures and components according to Douglas et al. (2011). Urban areas in Asia offer good examples of new forms of suburbs with emphasis on high-rise apartment buildings interspersed with managed green spaces. Singapore, for instance, has developed an island-wide park connector network designed to meet the perceived growing need for a variety of alternative recreational facilities. Green corridors at least 20 m wide link these open spaces. The highly urbanized island has planned its parks and open spaces to optimize the use of limited land and resources (Tan, 2006). Similar approaches can be seen in some newer urban developments in China (Kong et al., 2010), and Mactan Island could be a model for the Philippines. A long-term development plan on the study area can be found in their Comprehensive Land Use Plan (CLUP), which is updated and reviewed every 5 years to provide direction for future activities over a 10- to 20-year period after plan adoption. The results of this study could provide the local government unit better information in identifying places such as provisions of green spaces that can be included in their CLUP. The provision of vegetation or green spaces to coexist with built-up areas could be achieved through proper planning and policy implementation by the local government with the cooperation and participation of the people of Lapu-Lapu City and Cordova.

CONCLUSION

As Mactan Island is a developing economy, there are still many limitations concerning data acquisition, analysis, interpretation, and use of geospatial data that are appropriate for urban land use and land cover planning. Nevertheless, a significant step towards progress has been made via this study. The rise of and access to recent technologies such as satellite imagery and open-source GIS software mean that data gathering and modeling scenarios pertinent to conservation and enhancement of urban environment become easier. Change in land cover in Mactan Island was observed using these data and tools. Inclusions of these methods in the local planning system will help decision makers better explain and interpret the implications of information derived from the data provided by these methods. Unlike any other cities in Cebu, the island has its limitations in land areas when it comes to urban expansion. The increasing population that stimulates rapid land cover change may threaten the carrying capacity of the island. LST change observed during the study period was found to correlate with LULC change. These findings provide a new understanding of the urbanization process in Mactan Island, Central Philippines, and can be used further to investigate the effect of LULC on local climate change in the future.

REFERENCES

Abdollahi, K. K., & Ning, Z. H. (2000, January 15). Urban vegetation and their relative ability in intercepting particle pollution (PM2.5) [Abstract]. In *Third Symposium on the Urban Environment* [Symposium]. UC Davis Campus, Davis, CA. https://ams.confex.com/ams/AugDavis/techprogram/paper_14284.htm

Aboelnour, M., & Engel, B. A. (2018). Application of remote sensing techniques and geographic information systems to analyze land surface temperature in response to land use/land cover change in Greater Cairo Region, Egypt. *Journal of Geographic Information System*, *10*, 57–88. https://doi.org/10.4236/jgis.2018.101003

Akbari, H., Rosenfeld, A., Taha, H., & Gartland, L. (1996). Mitigation of summer urban heat islands to save electricity and smog. In *Proceedings of the 76th Annual American Meteorological Society Meeting. Atlanta, GA, 28 January–2 February 1996* (Report No. LBL-37787). Berkeley, CA: Lawrence Berkeley National Laboratory.

Akbari, H., Pomerantz, M., & Taha, H. (2001). Cool surfaces and shade trees to reduce energy use and improve air quality in urban areas. *Solar Energy*, *70*(3), 295–310.

Allen, N., Haarhoff, E., & Beattie, L. (2018) Enhancing liveability through urban intensification: The idea and role of neighbourhood. *Cogent Social Sciences*, *4*, 1. https://doi.org/10.1080/23311886.2018.1442117

Alwahiti, R. H., & Mitsova, D. (2016). Using Landsat-8 data to explore the correlation between urban heat island and urban land uses. *International Journal of Research in Engineering and Technology*, *5*(3), 457–466.

Alphan, H. (2003). Land use change and urbanization of Adana, Turkey. *Land Degradation & Development*, *14*(6), 575–586.

Busato, R. M., Lazzarin, M. N., & Noro, M. (2014). Three years of study of the urban heat island in Padua: Experimental results. *Sustainable Cities and Society*, *10*, 251–258.

Bhatta, B. (2010). *Analysis of urban growth and sprawl from remote sensing*. Springer-Verlag Berlin Heidelberg.

https://doi.org/10.1007/978-3-642-05299-6

Brody, S. (2013). The characteristics, causes, and consequences of sprawling development patterns in the United States. *Nature Education Knowledge*, *4*(5), 2.

Chavez, P. S. (1996). Image-based atmospheric corrections—Revisited and improved. *Photogrammetric Engineering and Remote Sensing*, *62*(9), 1025–1036.

Congedo, L. (2016). *Semi-Automatic Classification Plugin documentation*. https://dx.doi.org/10.13140/RG.2.2.29474.02242/1

Dewan, A. M., & Yamaguchi, Y. (2009). Land use and land cover change in Greater Dhaka, Bangladesh: Using remote sensing to promote sustainable urbanization. *Applied Geography*, *29*, 390–401.

Douglas, I., Goode, D., Houck, M., & Wang, R. (Eds.). (2011). *The Routledge Handbook of Urban Ecology*. Abingdon, Oxon, UK: Routledge.

EPA (US Environmental Protection Agency). (2008). Reducing urban heat islands: Compendium of strategies. Washington, DC: US Environmental Protection Agency.

Estoque, R. C., Murayama, Y., & Myint, S. W. (2017). Effects of landscape composition and pattern on land surface temperature: An urban heat island study in the megacities of Southeast Asia. *Science of the Total Environment*, *577*, 349–359. https://doi.org/10.1016/j.scitotenv.2016.10.195

FAO, & FAPDA. (2015). Country fact sheet on food and agriculture policy trends: Socio-economic context and role of agriculture. https://www.fao.org/economic/fapda/tool

Faridatul, M. I. (2017). Spatiotemporal effects of land use and river morphological change on the microclimate of Rajshahi Metropolitan Area. *Journal of Geographic Information System*, *9*, 466–481. https://doi.org/10.4236/jgis.2017.94029

Fuller, R. A., Irvine, K. N., Devine-Wright, P., Warren, P. H., & Gaston, K. J. (2007). Psychological benefits of greenspace increase with biodiversity. *Biological Letters*, *3*(4), 390–394.

Global Administrative Areas. (2012). *GADM database of Global Administrative Areas, version 2.0*. https://www.gadm.org

Global Visualization (GloVis) Viewer. (2005). Reston, VA: U.S. Department of the Interior, U.S. Geological Survey.

Ilieva, R. T. (2017). Urban food systems strategies: A promising tool for implementing the SDGs in practice. *Sustainability*, *9*(10), 1–35. https://doi.org/10.3390/su9101707

Jacquin, A., Misakova, L., & Gay, M. (2008). A hybrid object-based classification approach for mapping urban sprawl in periurban environment. *Landscape and Urban Planning*, *84*, 152–165.

Jung, M. (2016). LecoS—A Python plugin for automated landscape ecology analysis. *Ecological Informatics*, *31*, 18–21. https://dx.doi.org/10.1016/j.ecoinf.2015.11.006

Kong, F., Yin, H., Nakagoshi, N., & Zong, Z. (2010). Urban green space network development for biodiversity conservation: Identification based on graph theory and gravity modeling. *Landscape and Urban Planning*, *95*(1–2), 16–27.

Lassila, K. D. (1999). The new suburbanites: How American plants and animals are threatened by the sprawl. *Amicus Journal*, *21*, 16–22.

Leitão, A. B., Miller, J., Ahern, J., & McGarigal, K. (2006). *Measuring landscapes: A planner's handbook*. Island Press.

Lopez, E., Bocco, G., Mendoza, M., & Duhau, E. (2001). Predicting land cover and land use change in the urban fringe. A case in Morelia City, Mexico. *Landscape and Urban Planning*, *55*(4), 271–285.

Miller, R. B., & Small, C. (2003). Cities from space: Potential application of remote sensing in urban environmental research and policy. *Environmental Science & Policy*, *6*(2), 129–137. https://doi.org/10.1016/S1462-9011(03)00002-9

Mitchell, R., & Popham, F. (2008). Effect of exposure to natural environment on health inequalities: An observational population study. *The Lancet*, *372*(9650), 1655–1660. https://doi.org/10.1016/S0140-6736(08)61689-X

NAMRIA. (1993). *Cebu City Quadrangle* (Sheet No. 3721-I). Taguig City, Metro Manila, Philippines: NAMRIA.

Nowak, D. J., Civerolo, K. L., Trivikrama Rao, S., Sistla, G., Luley, C. J., & Crane, D. E. (2000). A modeling study of the impact of urban trees on ozone. *Atmospheric Environment*, *34*(10), 1601–1613.

Oke, T. R. (1982). The energetic basis of the urban heat island. *Quarterly Journal of the Royal Meteorological Society*, *108*(455), 1–24.

Olofsson, P., Foody, G. M., Herold, M., Stehman, S. V., Woodcock, C. E., & Wulder, M. A. (2014). Good practices for estimating area and assessing accuracy of land change. *Remote Sensing of Environment*, *148*, 42–57.

Pretty, J., Peacock, J., Hine, R., Sellens, M., South, N., & Griffin, M. (2007). Green exercise in the UK countryside: Effects on health and psychological well-being, and implications for policy and planning. *Journal of Environmental Planning and Management*, *50*(2), 211–231.

PSA. (2000). *Philippine Statistics Authority. Census of Population (2015). Region VII (Central Visayas).* https://psa.gov.ph/content/2000-census-population-and-housing-highlights-preliminary-results

PSA. (2015). *Philippine Statistics Authority. Census of Population (2015). Region VII (Central Visayas).* https://psa.gov.ph/content/population-region-vii-central-visayas-based-2015-census-population

QGIS Development Team. (2015). *QGIS Geographic Information System*. Open Source Geospatial Foundation Project. https://qgis.osgeo.org

Rahman, M. R., & Saha, S. K. (2007). Multi-resolution segmentation for object-based classification and accuracy assessment of land use/land cover classification using remotely sensed data. *Journal of the Indian Society of Remote Sensing*, *36*, 189–201.

Sabins, F. F. (1996). *Remote sensing: Principles and interpretation* (3rd ed.). New York: W. H. Freeman and Company.

Sobrino, J. A., Jiménez-Muñoz, J. C., & Paolini, L. (2004). Land surface temperature retrieval from LANDSAT TM 5. *Remote Sensing of Environment*, *90*, 434–440.

Son, N. T., & Thanh, B. X. (2017). Decadal assessment of urban sprawl and its effects on local temperature using Landsat data in Cantho City, Vietnam. *Sustainable Cities and Society*, *36*, 81–91. https://doi.org/10.1016/j.scs.2017.10.010

Susca, T., Gaffin, S. R., & Dell'Osso, G. R. (2011). Positive effects of vegetation: Urban heat island and green roofs. *Environmental Pollution*, 159(8–9), 2119–2126.

Takebayashi, H., & Moriyama, M. (2007). Surface heat budget on green roof and high reflection roof for mitigation of urban heat island. *Building and Environment*, *42*(8), 2971–2979.

Tan, K. W. (2006). A greenway network for Singapore. *Landscape and Urban Planning*, *76*(1–4), 45–66.

Tao, C., & Xin, L. (2004). Retrieval of snow depth in China by passive microwave remote sensing data and its accuracy assessment. *Remote Sensing Technology and Application*, *19*(5), 301–306. https://doi.org/10.11873/j.issn.1004-0323.2004.5.301

Tefft, J., Jonasova, M., Adjao, R., & Morgan, A. (2017). *Food systems for an urbanizing world*. World Bank and FAO.

Tsai, Y.-H. (2005). Quantifying urban form: Compactness versus 'sprawl.' *Urban Studies*, *42*, 141–161.

Turner, B. L., II. (1994). Local faces, global flows: The role of land use and land cover in global environmental change. *Land Degradation and Rehabilitation*, *5*, 71–78.

Twum, K. O., & Ayer, J. (2019). Connecting the complex dots: A review of urban change complexities in Ghana. *Cogent Social Sciences*, *5*, 1. https://doi.org/10.1080/23311886.2019.1677119

USGS. (2016). *Landsat 8 (L8): Data users handbook version 2*. Sioux Falls, SD: EROS, Department of the Interior U.S. Geological Survey. https://www.usgs.gov/media/files/landsat-8-data-users-handbook

Wagrowski, D. M., & Hites, R. A. (1997). Polycyclic aromatic hydrocarbon accumulation in urban, suburban and rural vegetation. *Environmental Science and Technology*, *31*(1), 279–282.

Wasserman, M. (2000). Confronting urban sprawl. In *Regional Review of the Federal Reserve Bank of Boston*. Boston, Massachusetts, USA.

Weng, Q., Lu, D., & Schubring, J. (2004). Estimation of land surface temperature-vegetation abundance relationship for urban heat island studies. *Remote Sensing of Environment*, *89*, 467–483.

Wilson, E. H., Hurd, J. D., Civco, D. L., Prisloe, M. P., & Arnold, C. (2003). Development of a geospatial model to quantify, describe and map urban growth. *Remote Sensing of Environment*, *86*(3), 275–285.

World Bank. (2007). *Dhaka: Improving living conditions for the urban poor* (Report No. 35824-BD). Sustainable Development Unit, South Asia Region.